

SEISMIC REHABILITATION DESIGN OF STEEL MOMENT CONNECTION WITH WELDED HAUNCH

By Qi-Song “Kent” Yu,¹ Student Member, ASCE, Chia-Ming Uang,² and John Gross,³ Members, ASCE

ABSTRACT: This paper describes a design procedure for the seismic rehabilitation of pre-Northridge steel moment connections using a welded haunch. Experimental results from cyclic testing of full-scale specimens demonstrated that welding a triangular haunch beneath the beam’s bottom flange significantly improved the seismic performance of steel moment connections. The welded haunch drastically changed the beam shear force transfer mechanism, which assisted in reducing the demands at the beam flange groove welds. Analytical studies further showed that the tensile stress in the existing beam flange groove weld can be reduced to a reasonable level if the flange of the haunch is designed to provide sufficient stiffness and strength. However, traditional beam theory cannot provide a reliable prediction of the beam’s flexural stress distribution near the column face. A simplified model that allows the designer to predict the stress level in the beam flange groove welds is presented.

INTRODUCTION

The Northridge, Calif., earthquake of January 17, 1994, resulted in widespread damage to beam-column connections in steel special moment-resisting frames. Because of this newly identified vulnerability to connection fracture in existing special moment-resisting frames, NIST, Gaithersburg, Md., and AISC, Chicago, initiated a research project to investigate the effectiveness of two rehabilitation schemes—reduced beam section and welded haunch schemes—for seismic rehabilitation (Civjan and Engelhardt 1998; Uang et al. 2000). When the complete joint penetration welded joint of the beam top flange was left in its pre-Northridge condition, test results showed that the welded haunch specimens performed better than the reduced beam section specimens. When a concrete slab was present, brittle fracture of groove welded joints was prevented. These full-scale specimens were able to provide large plastic rotation in a ductile manner.

For seismic rehabilitation purposes, the welded haunch scheme not only provides a more redundant moment connection but also eliminates the need to modify the existing groove weld of the top flange, indicating a potential for significant cost savings. In this paper, test results that support the effectiveness of the welded haunch scheme are presented first. Next, it is shown that conventional beam theory cannot provide a reliable prediction of the flexural stresses in the groove welded joint. Third, a simplified model that considers the interaction of forces and deformation compatibility between the beam and the haunch is developed. Finally, a step-by-step design procedure is presented. The proposed design procedure is demonstrated by an example in Appendix I.

AVAILABLE TEST RESULTS

In this NIST/AISC research program, two different sizes of full-scale welded haunch specimens were tested. Two large-

¹Grad. Res. Asst., Dept. of Struct. Engrg., Univ. of California at San Diego, La Jolla, CA 92093-0085.

²Assoc. Prof., Dept. of Struct. Engrg., Univ. of California at San Diego, La Jolla, CA.

³Build. and Fire Res. Lab., Nat. Inst. of Standards and Technol., Gaithersburg, MD 20899.

Note. Associate Editor: Takeru Igusa. Discussion open until June 1, 2000. Separate discussions should be submitted for the individual papers in this symposium. To extend the closing date one month, a written request must be filed with the ASCE Manager of Journals. The manuscript for this paper was submitted for review and possible publication on March 2, 1999. This paper is part of the *Journal of Structural Engineering*, Vol. 126, No. 1, January, 2000. ©ASCE, ISSN 0733-9445/00/0001-0069-0078/\$8.00 + \$.50 per page. Paper No. 20492.

size, two-sided moment connection specimens consisting of W36×150 beams, W14×426 column, and a triangular haunch cut from a W14×143 section were tested at the University of California at San Diego (UCSD) (Uang et al. 2000), and another four medium-size specimens consisting of W30×99 beams, W12×279 column, and a W21×93 haunch were tested at the University of Texas, Austin (Civjan and Engelhardt 1998). Fig. 1 summarizes the test results. Of the three bare steel specimens tested, five beams experienced brittle fracture of groove weld in the top flange. When the concrete slab was present, none of the six beams experienced weld fracture, and the plastic rotation ranged from 0.028 to 0.031 rad, which has been considered adequate for rehabilitation purposes (“Interim” 1995).

NUMERICAL SIMULATION OF HAUNCH CONNECTION

To gain more insight into the behavior of the welded haunch connection, one bare steel specimen that was tested at UCSD was modeled and analyzed using the general-purpose finite-element analysis program ABAQUS (ABAQUS 1995). Both flanges and the web of the beams and the column were modeled with the quadrilateral four-node shell element (element type S4R5 in ABAQUS). Each element was divided into five layers across the thickness so that the stress gradient could be modeled. A reduced integration scheme with one Gaussian integration point in the center of each layer was used to for-

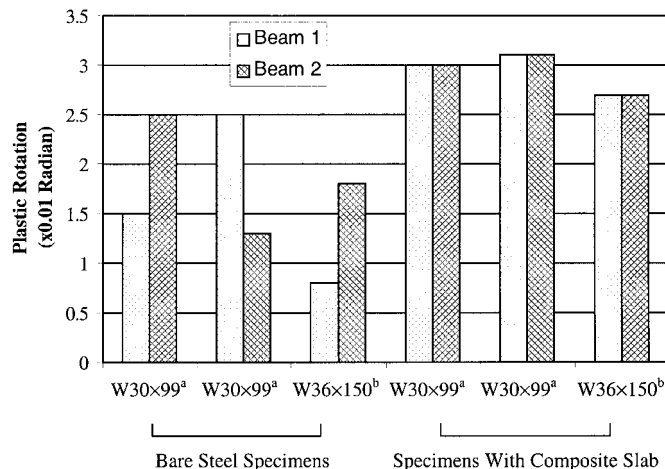


FIG. 1. Plastic Rotation Capacities of NIST/AISC Welded Haunch Specimens [a: from Civjan and Engelhardt (1998); b: from Uang et al. (2000)]

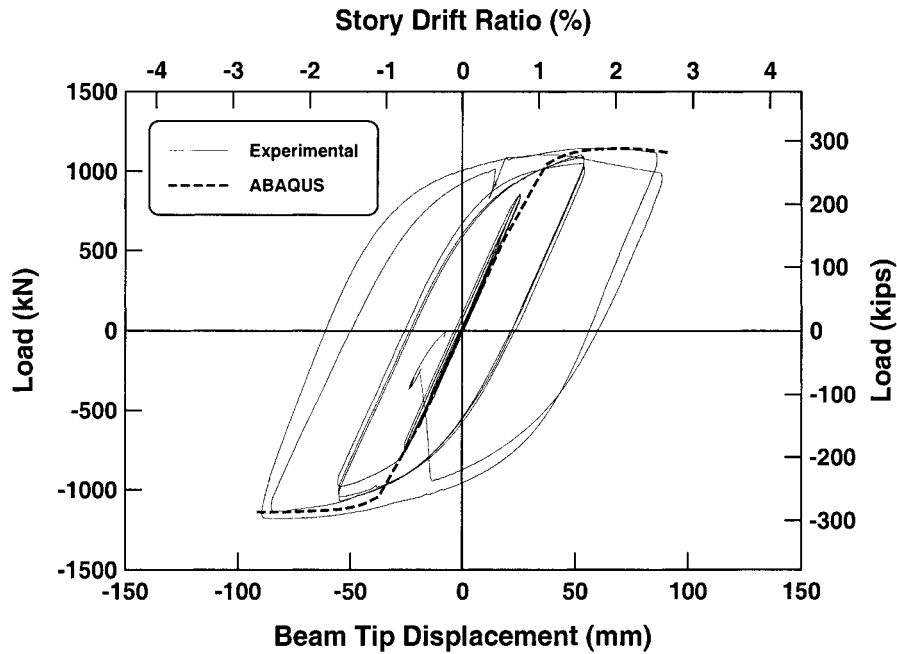


FIG. 2. Correlation of Analytical and Experiment Load-Displacement Relationships

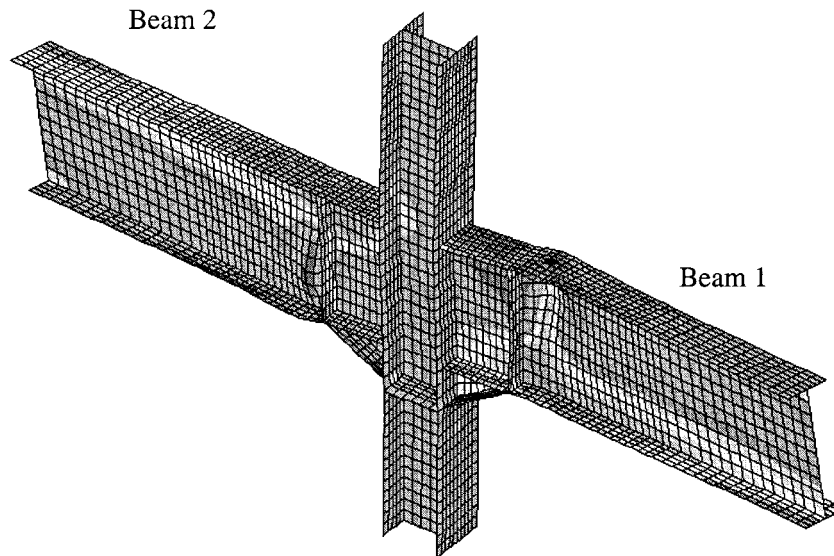


FIG. 3. Deformed Configuration of Welded Haunch Specimen

simulate element properties. The beam web was directly connected to the column flange in the model. Steel material properties followed the results of tension coupon tests; a Young's modulus of 199,955 MPa (29,000 ksi) and a Poisson's ratio of 0.3 were assumed. The material was assumed to be elastic-plastic, which followed the von Mises yielding criterion. Equal and opposite displacements were imposed to the beam ends.

An updated Lagrangian formulation, Green's strain, and second Piola-Kirchhoff stress were used to account for the effect of large displacements and finite strains. To simulate the strength degradation due to local buckling and lateral-torsional buckling, the standard Newton method, which fails (i.e., diverges numerically) near the maximum strength point of the force-displacement curve, was not adopted for the analysis. Instead, the modified Riks algorithm (Ramm 1981) was used so that the postbuckling behavior could be predicted.

Fig. 2 shows that the analytically predicted load versus beam tip deflection relationship correlated well with the response envelope of the test results. The predicted deformation

configuration is shown in Fig. 3. Under positive bending, Beam 1 experiences not only local buckling in the flange and the web but also lateral-torsional buckling. Beam 2 under negative bending also experiences local and lateral-torsional buckling, but the buckling amplitudes are significantly smaller than those of Beam 1. Based on this satisfactory correlation study, the finite-element model was then used to compute the stress distributions of the welded haunch connection.

SHEAR FORCE TRANSFER AND INTERNAL STRESS DISTRIBUTIONS

Consider this UCSD test specimen as an example. Based on an elastic ABAQUS analysis, the flexural stress distribution along the beam section near the column face is presented in Fig. 4. For comparison purposes, the stress profile based on a simple beam theory (i.e., My/I_{bb} , where M is the moment, y is the distance measured from the elastic neutral axis, and I_{bb} is the moment of inertia of the composite section) is also shown. The poor correlation between the stress distributions is obvious.

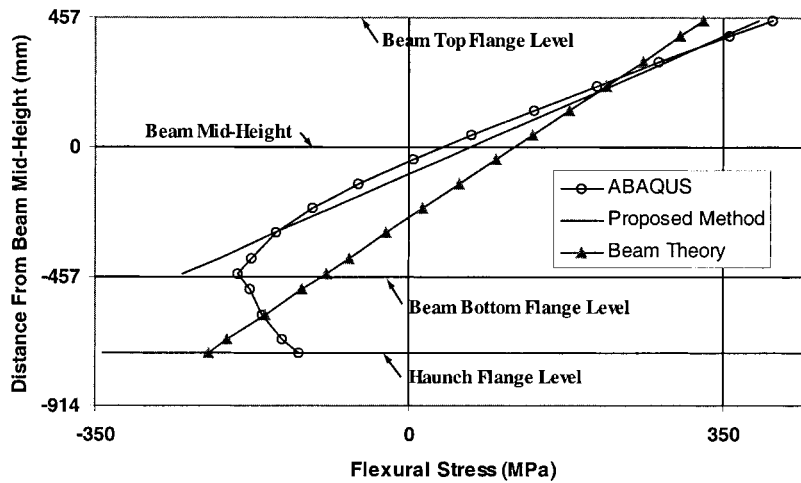


FIG. 4. Comparison of Flexural Stress Profiles along Beam Depth

Without the welded haunch, it has been shown that the majority of the beam shear is transferred to the column through beam flanges, not the beam web (Popov and Stephen 1972; Goel et al. 1997; El-Tawil et al. 1998). When the haunch is present, the majority of the beam shear is transferred through the haunch flange acting as a strut action to the column. When the axial stiffness of the haunch flange is sufficiently stiff, the direction of the beam web shear in the haunch-reinforced region can be even reversed. Such a reversed shear phenomenon was also observed from experimental testing (Uang et al. 2000). Needless to say, the simple beam theory could not predict this reversed shear phenomenon.

SIMPLIFIED MODEL OF WELDED HAUNCH CONNECTION

In this section, a mathematical model that considers the interaction (i.e., force equilibrium and deformation compatibility) between the beam and the haunch is presented.

Beam Moment Diagram

Fig. 5 shows the simplified model of the welded haunch connection, where the haunch flange is idealized as a spring. The contribution of the haunch web to the stiffness in the haunch flange direction is minor and can be ignored. (A numerical study of the UCSD test specimen showed that the haunch web increased the haunch stiffness by about 5%.) At the haunch tip, the amount of beam shear force that is transferred to the haunch flange is dependent on the axial stiffness of the haunch flange.

Let the vertical component of the haunch flange axial force be βV_{pd} , where V_{pd} is the beam shear at the inflection point of the beam and β remains to be established [Fig. 6(a)]. The horizontal component of the haunch flange force is then equal to $\beta V_{pd} / \tan \theta$. Such a horizontal force component together with an eccentricity of $d/2$ (due to the finite depth of the beam) produces a tensile force and a concentrated moment to the beam in the haunch region [Fig. 6(b)]. Fig. 6(c) shows the moment diagram of the beam alone. The seismic beam moment increases from zero at the inflection point to a peak moment of $V_{pd}L'/2$ at the haunch tip location. The moment at that location is reduced by the concentrated moment, $(\beta V_{pd} / \tan \theta)(d/2)$, shown in Fig. 6(b).

The variation of the beam moment diagram inside the haunch region then reflects the beam shear. If β is equal to 1 [i.e., all the beam shear V_{pd} is transmitted to the haunch flange], the beam shear in the haunch region vanishes, and the beam moment would be constant in that region. When β is

larger than 1, the beam shear in the haunch region is reversed in direction as compared with that outside the haunch region. Because beam shear is the slope of the moment diagram, the reverse shear would further reduce the beam moment and, hence, the tensile stress in the top groove weld at the column face [Fig. 6(c)].

Deformation Compatibility between Beam and Haunch

Consider the beam free-body shown in Fig. 6(a). The horizontal and vertical components of the beam deformation at

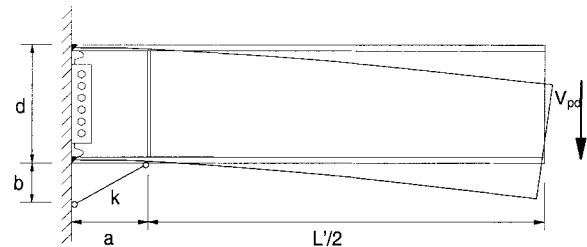


FIG. 5. Simplified Model of Welded Haunch Connection

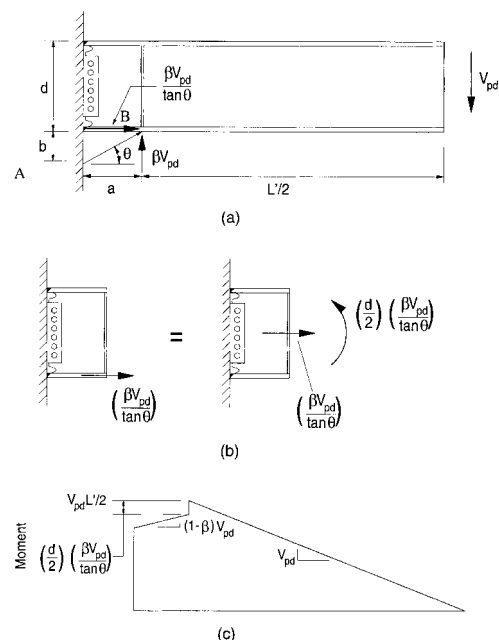


FIG. 6. Free Body and Moment Diagram of Haunch Reinforced Beam: (a) Free Body Diagram of Beam; (b) Eccentric Force due to Strut Action; (c) Reduction of Moment due to Eccentric Force

the haunch tip (Point B) can be computed as follows. Define x in Fig. 6(a) as the distance of the beam section measuring from the haunch tip toward the column face. The beam bending moment in the haunch region [Fig. 6(c)] is

$$M(x) = \left(\frac{L'}{2} + x\right) V_{pd} - x(\beta V_{pd}) - \left(\frac{\beta V_{pd}}{\tan \theta}\right) \frac{d}{2} \quad (1)$$

(See Appendix III for the notations.) This bending moment together with the beam axial force [$\beta V_{pd}/\tan \theta$ in Fig. 6(b)] produces a compressive stress in the beam bottom flange as follows:

$$\sigma(x) = \frac{(L'/2 + x)V_{pd}}{I_b} \left(\frac{d}{2}\right) - \frac{x(\beta V_{pd})}{I_b} \left(\frac{d}{2}\right) - \frac{(\beta V_{pd}/\tan \theta)}{I_b} \left(\frac{d}{2}\right)^2 - \frac{\beta V_{pd}/\tan \theta}{A_b} \quad (2)$$

The horizontal component u_B of the beam deformation at the haunch tip is equal to the axial shortening of the beam bottom flange in the haunch region

$$u_B = \int_0^a \frac{\sigma(x)}{E} dx = \left(\frac{L'/d - (\beta/\tan \theta)}{EI_b}\right) \left(\frac{d}{2}\right)^2 a + \frac{(1 - \beta)a^2}{2EI_b} \left(\frac{d}{2}\right) - \frac{\beta a/\tan \theta}{EA_b} V_{pd} \quad (3)$$

Next, consider the vertical component of the beam deformation at the haunch tip. Using the moment-area method, where the moment is expressed in (1), the vertical component is

$$v_B = \int_0^a \frac{xM(x)}{EI_b} dx = \left(\frac{L'/d - (\beta/\tan \theta)}{EI_b}\right) \left(\frac{d}{4}\right) a^2 + \frac{(1 - \beta)a^3}{3EI_b} V_{pd} \quad (4)$$

Based on the components u_B and v_B of the haunch tip displacement, the shortening of the haunch flange δ_h is

$$\delta_h = \sqrt{(a - u_B)^2 + (b - v_B)^2} - l_{hf} \approx u_B \cos \theta + v_B \sin \theta \quad (5)$$

where $b (=a \tan \theta)$ = haunch depth; and $l_{hf} (=a/\cos \theta)$ = haunch flange length. Based on the small deformation theory, a simplification was made in (5) by ignoring higher-order terms.

The axial shortening of the haunch flange can also be established by considering the haunch flange as a free body. Because the vertical component of the haunch flange force is βV_{pd} , the axial force in the haunch flange is equal to $\beta V_{pd}/\sin \theta$, and the corresponding axial shortening is

$$\delta_h = \frac{\beta V_{pd}}{EA_{hf} \sin \theta} l_{hf} \quad (6)$$

Equating (5) and (6) for deformation compatibility gives

$$u_B \cos \theta + v_B \sin \theta = \frac{\beta V_{pd}}{EA_{hf} \sin \theta} l_{hf} \quad (7)$$

Solving the above equation for β yields the following expression:

$$\beta = \frac{b}{a} \left(\frac{3L'd + 3ad + 3bL' + 4ab}{3d^2 + 6bd + 4b^2 + \frac{12I_b}{A_b} + \frac{12I_b}{A_{hf} \cos^3 \theta}} \right) \quad (8)$$

The above equation defines the interface force coefficient between the beam and the haunch flange.

TENSILE STRESSES IN BEAM FLANGE GROOVE WELDS

Because the majority of the beam shear is transferred through the haunch flange to the column, for design purposes,

the beam top flange stress (i.e., the tensile stress in the groove weld) at the column face can be calculated by beam theory as follows:

$$f_{wt} = \frac{V_{pd}(L'/2 + a)}{I_b} \left(\frac{d}{2}\right) - \frac{\beta V_{pd}a}{I_b} \left(\frac{d}{2}\right) - \frac{(\beta V_{pd}/\tan \theta)(d/2)}{I_b} \left(\frac{d}{2}\right) + \frac{\beta V_{pd}/\tan \theta}{A_b} = \frac{V_{pd}L'/2 + V_{pd}(1 - \beta)a}{I_b} \left(\frac{d}{2}\right) - \frac{(\beta V_{pd}/\tan \theta)}{I_b} \left(\frac{d^2}{4} - \frac{I_b}{A_b}\right) \quad (9)$$

Defining M_{pd} as the design moment of the beam at the haunch tip, the corresponding beam shear V_p is equal to $M_{pd}/(L'/2)$. Substituting the bending moment $V_{pd}/L'/2$ at the haunch tip by M_{pd} , the above equation can be rewritten as follows:

$$f_{wt} = \frac{M_{pd} + V_{pd}(1 - \beta)a}{I_b} \left(\frac{d}{2}\right) - \frac{\beta V_{pd}/\tan \theta}{I_b} \left(\frac{d^2}{4} - \frac{I_b}{A_b}\right) \quad (10)$$

Based on Fig. 7(b), the beam bottom flange force P_{bf} , to the left of the haunch tip (Point B) is much smaller than that in the top flange due to the contribution of the horizontal component of the haunch flange force [Fig. 6(b)]. To compute the maximum tensile stress in the beam bottom flange groove weld when the beam is subjected to positive bending [i.e., when V_{pd} in Fig. 6(a) acts upward], the following equation can be derived with minor modifications of (9):

$$f_{wb} = \frac{V_{pd}(L'/2 + a)}{I_b} \left(\frac{d}{2}\right) - \frac{\beta V_{pd}a}{I_b} \left(\frac{d}{2}\right) - \frac{(\beta V_{pd}/\tan \theta)(d/2)}{I_b} \left(\frac{d}{2}\right) - \frac{\beta V_{pd}/\tan \theta}{A_b} = \frac{V_{pd}L'/2 + V_{pd}(1 - \beta)a}{I_b} \left(\frac{d}{2}\right) - \frac{(\beta V_{pd}/\tan \theta)}{I_b} \left(\frac{d^2}{4} + \frac{I_b}{A_b}\right) \quad (11)$$

The flexural stress profiles of the beam based on (10) and (11) are compared with those predicted by the simple beam theory and the finite-element analysis in Fig. 4. Good correlation between the proposed model and the finite-element model indicates that (10) and (11) can be used reliably for design purposes.

The axial deformation of the haunch flange would result in secondary shear stresses in the haunch web due to the deformation compatibility between the haunch flange and the haunch web (Fig. 8). Treating the triangular haunch web as a first-order finite element, the shear strain is

$$\gamma_{hw} = \frac{\partial u(x, y)}{\partial y} + \frac{\partial v(x, y)}{\partial x} \quad (12)$$

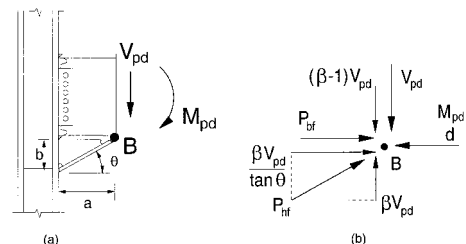


FIG. 7. Force Equilibrium at Haunch Tip: (a) Free Body; (b) Force Equilibrium

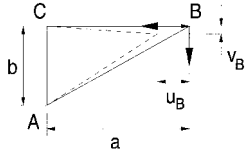


FIG. 8. Deformation of Haunch Web

where the displacement fields $u(x, y)$ and $v(x, y)$ can be expressed as a function of the nodal displacements u_B and v_B at the haunch tip

$$u(x, y) = \left(1 - \frac{x}{a}\right) u_B \quad (13)$$

$$v(x, y) = \left(1 - \frac{x}{a}\right) v_B \quad (14)$$

Substituting (13) and (14) into (12) gives the following:

$$\gamma_{hw} = -\frac{v_B}{a} \quad (15)$$

Substituting (4) for v_B and multiplying both sides of the above equation by the shear modulus $[E/2(1 + \nu)]$ gives the following shear stress in haunch web:

$$\begin{aligned} \tau_{hw} &= \frac{E}{2(1 + \nu)} \left(\frac{L'/2 - (\beta/\tan \theta) \frac{d}{2}}{EI_b} V_{pd} a + \frac{(1 - \beta)a^2}{3EI_b} V_{pd} \right) \\ &= \frac{aV_{pd}}{2.6I_b} \left(\frac{L'}{2} - \frac{\beta}{\tan \theta} \left(\frac{d}{2}\right) + \frac{(1 - \beta)a}{3} \right) \end{aligned} \quad (16)$$

where $\nu(0.3) =$ Poisson's ratio.

SIZING HAUNCH FLANGE

For economic reasons, it is not desirable to modify the existing beam flange groove welds. The NIST/AISC test results have shown that brittle fracture of the beam top flange groove weld did not occur when the composite slab was present even though strain gauge measurements indicated that the beam top flange not only yielded but also strain-hardened. Based on strain gauge measurements of the welded haunch specimens, the beam top flange strain near the column face was found to approach 20–30 times the yield strain. Since the actual yield stress of the beam flange for the UCSD specimens was about 338 MPa (49 ksi), the tensile stress in the beam top flange and its groove weld (with the E7XT-X electrode) might have exceeded 379 MPa (55 ksi) due to strain hardening under cyclic loading. Therefore, it is recommended that the allowable stress F_w , in an average sense across the beam flange area, for the existing groove welds be taken as $0.8F_{EXX}$, where F_{EXX} is the strength of the weld metal (Gross et al. 1999). For a 483 MPa (70 ksi) tensile strength electrode, this requirement would limit the allowable stress in the groove weld to $0.8(483) = 386$ MPa (56 ksi).

When sizing the haunch flange to limit f_w to the allowable stress, the minimum value of β can be solved by equating (10) to the average allowable weld stress F_w

$$\beta_{\min} = \frac{(M_{pd} + V_{pd}a)/S_x - F_w}{\frac{V_{pd}a}{S_x} + \frac{V_{pd}}{I_b \tan \theta} \left(\frac{d^2}{4} - \frac{I_b}{A_b}\right)} \quad (17)$$

The haunch flange axial force P_{hf} is equal to $\beta V_{pd}/\sin \theta$, and once the minimum value of βV_{pd} is determined, the haunch flange can be sized as follows:

$$A_{hf} \geq \frac{P_{hf}}{\phi F_y} = \frac{\beta V_{pd}}{\phi F_y \sin \theta} \quad (18)$$

where $A_{hf} =$ haunch flange area $= b_{hf} t_{hf}$; $b_{hf} =$ haunch flange width; $t_{hf} =$ haunch flange thickness; $\phi = 0.9$, and $F_y =$ minimum specified yield stress of the haunch flange. The haunch flange should satisfy the following width-thickness requirement for a compact section (Seismic 1997):

$$\frac{b_{hf}}{2t_{hf}} \leq \frac{137}{\sqrt{F_y}} \text{ (SI units)} \quad \text{or} \quad \frac{b_{hf}}{2t_{hf}} \leq \frac{52}{\sqrt{F_y}} \text{ (U.S. units)} \quad (19)$$

In addition to satisfying the strength requirement in (18) and the stability requirement in (19), it is necessary to check the axial stiffness of the selected haunch flange to ensure that the actual β value, as computed from (8), is not less than β_{\min} . If the haunch flange is conservatively designed, the actual β value will be significantly larger than β_{\min} . In such a case, the designer may consider reducing the haunch flange area.

SIZING HAUNCH WEB

Note that the contribution of the haunch web is excluded in the force equilibrium in Fig. 7(b) because its stiffness in the haunch flange direction is small. However, the haunch web plays an important role in providing stability for the haunch flange. For design purposes, it is suggested that the thickness of the haunch web satisfy the following requirement:

$$\frac{a \sin \theta}{t_{hw}} \leq \frac{683}{\sqrt{F_y}} \text{ (SI units)} \quad \text{or} \quad \frac{a \sin \theta}{t_{hw}} \leq \frac{260}{\sqrt{F_y}} \text{ (U.S. units)} \quad (20)$$

The above requirement is established by treating the haunch as half of a wide-flange beam section whose depth is twice the distance of $a \sin \theta$ in Fig. 9; the limiting width-thickness ratio, $2a \sin \theta/t_{hw}$, would be $1,365/\sqrt{F_y}$ (or $520/\sqrt{F_y}$ in U.S. units) in accordance with AISC's Seismic Provisions for Structural Steel Buildings.

The shear stress in the haunch web, as computed from (16), should not exceed the allowable shear stress

$$\tau_{hw} \leq \phi_v(0.6F_y) \quad (21)$$

where $\phi_v = 0.9$.

OTHER DESIGN CONSIDERATIONS

Preliminary Haunch Geometry

In the tests conducted to date, two geometrical parameters for the majority of test specimens, a and θ (Fig. 9), have varied only to a small extent. Until more test data become available, it is prudent to remain within the limits of experimental database. To begin a trial design, it is suggested that the length a and angle θ of the haunch be taken as (Gross et al. 1999)

$$a = (0.5 \text{ to } 0.6)d \quad (22)$$

$$\theta = 30^\circ \pm 5^\circ \quad (23)$$

The designer may want to check the value of $b (=a \tan \theta)$ to ensure that the haunch does not interfere with the ceiling and other nonstructural elements.

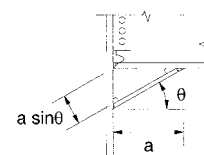


FIG. 9. Compactness Requirement for Haunch Web

Beam Design Plastic Moment and Shear Force

The design of a welded haunch is based on the moment and shear that develop at the tip of the haunch when the beam hinges plastically (SAC 1996). The design beam moment M_{pd} at the location of the haunch tip is computed as follows:

$$M_{pd} = \alpha Z_b F_{ye} \quad (24)$$

with α = material overstrength factor; Z_b = beam plastic modulus; and F_{ye} = expected yield strength of the beam.

Expected Yield Strength of Steel

The value of F_{ye} may be obtained from tensile tests of material removed from the existing building, from mill certification reports for the steel used in the construction, or from compiled statistical data. For the latter case, AISC's Seismic Provisions for Structural Steel Buildings (Seismic 1997) for new construction uses the following formula to compute the expected yield strength:

$$F_{ye} = R_y F_y \quad (25)$$

where R_y = multiplier established from statistical data to account for material overstrength (1.5 for A36 steel). For seismic rehabilitation, however, it is suggested that this value be adjusted in recognition of differences in mill practices that occurred around 1990. For steels produced after 1990, the value of $R_y = 1.5$ reflects the mill practice of dual certification whereby a single material is produced that meets the requirements of both ASTM A36 and A572 Grade 50. Steels produced before this practice is likely to have an expected yield strength considerably less than might be found today and a lower value of R_y may be justified. Thus, for steels produced prior to 1990, the value of $R_y = 1.3$ is suggested. This value is based on a statistical study of the results of over 7,500 tests on A7 and A36 steels (Galambos and Ravindra 1978) and adjusted upward for added safety (Gross et al. 1999).

Material Overstrength Factor

To obtain the value of α for (24), available welded haunch test data were analyzed and the results are shown in Fig. 10. Two plots are presented for two beam sizes: W30×99 and W36×150. The abscissa represents the story drift ratio (SDR), and the ordinate is the normalized moment. The beam moment is computed at the haunch tip location and the normalization is based on the actual plastic moment of the beam, where the yield stresses of A36 steel beams were obtained from tension coupon tests. It is observed that the beam probable plastic moment can be slightly larger than the actual plastic moment, and using a value of 1.1 for α is reasonable for design purposes.

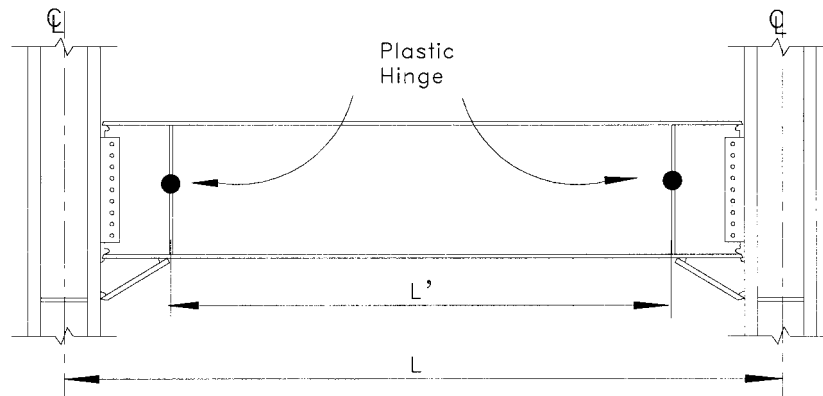


FIG. 11. Assumed Location of Beam Plastic Hinge

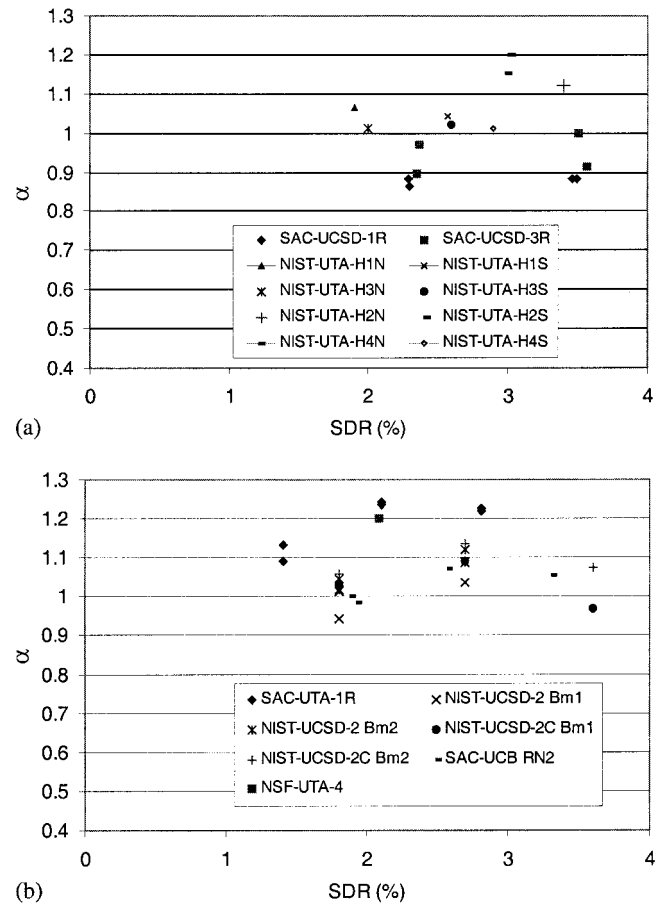


FIG. 10. SDR versus Moment Ratio: (a) W30×99 Beams; (b) W36×150 Beams

Once M_{pd} is determined, the corresponding beam shear V_{pd} can be computed as follows:

$$V_{pd} = \frac{2M_{pd}}{L'} + V_G \quad (26)$$

where L' = beam span between plastic hinges (Fig. 11); and V_G = beam shear at the plastic hinge location produced by gravity load in beam span L' .

Strong Column-Weak Beam Condition

The strong column-weak beam criterion should be checked when a haunch is welded to the pre-Northridge moment connection. Before a designer proceeds with the detailed design, information on the haunch length and angle is sufficient to check this criterion ("Interim" 1995)

$$\frac{\sum Z_c(F_{yc} - f_a)}{\sum M_c} > 1.0 \quad (27)$$

where Z_c = plastic section modulus of the column above and below the connection; F_{yc} = minimum specified yield stress for the column above and below; f_a = axial stress in the column above and below; and M_c = sum of column moments at the top and bottom ends of the enlarged panel zone resulting from the development of the probable beam plastic moment M_{pd} within each beam that frames into the connection. It can be computed as follows (Fig. 12):

$$\sum M_c = [2M_{pd} + V_{pd}(L - L')] \left(\frac{H_c - d_p}{H_c} \right) \quad (28)$$

Dual Panel Zone Shear Strength

The presence of a haunch also creates an enlarged (or “dual”) panel zone. Usually the increase in the panel zone shear strength is larger than the increase in shear demand; therefore, a check of panel zone strength is usually unnecessary. If desired, the designer can use the procedure developed by Lee and Uang (1997) to compute the shear strength of the dual panel zone.

Shear Strength of Existing Beam Web Connection

The beam shear is computed as follows. From the slope of the beam moment diagram (i.e., beam shear) in Fig. 6(c), it is observed that a shear of magnitude $(1 - \beta)V_{pd}$ in the direction of the beam shear outside the haunch is developed in the haunch region; the direction of this beam shear is opposite to that developed outside the haunch region if β is larger than 1. Therefore, the shear force in the beam web is

$$V_{bw} = (1 - \beta)V_{pd} \quad (29)$$

In general, the value of V_{bw} is significantly less than that of V_{pd} , indicating that the existing beam flange groove welds and the beam web connection only need to transfer a small amount of the shear force. If the value of V_{bw} is negative, it means that the direction of the beam shear in the haunch region is reversed. If the existing beam web connection does not have a sufficient capacity to resist V_{bw} , additional welding of the beam web to the shear plate may be required to increase the shear capacity.

Weld Design

A groove weld with a specified Charpy V-notch toughness of 27.1 J (20 ft-lb) at -28.8°C (-20°F) should be used to connect the haunch flange to both the column and beam

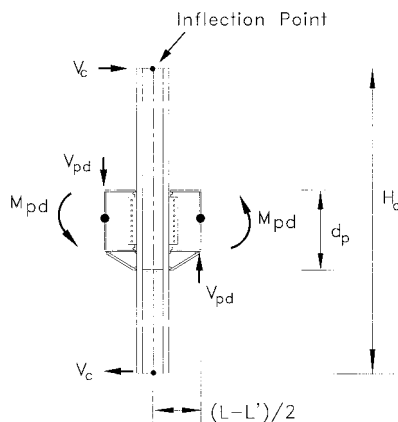


FIG. 12. Evaluation of Strong Column-Weak Beam Criterion

flanges (Seismic 1997). Connections between the haunch web and both the column and beam flanges should have sufficient strength per unit length to resist the following shear force:

$$V_{hw} = \tau_{hw} t_{hw} \quad (30)$$

Beam Web Transverse Stiffeners

The haunch flange exerts a concentrated force on the beam. Therefore, it is suggested that a pair of transverse stiffeners be added to the beam web at the location where the haunch flange intersects the beam. At a minimum, the stiffeners should extend at least half of the beam depth, and the width-to-thickness of each stiffener should be limited to $249/\sqrt{F_y}$ (or $95/\sqrt{F_y}$ in U.S. units). Such a measure would ensure that the vertical reaction βV_{pd} at the haunch tip would not be reduced by the flexibility of the beam web. Using full-depth stiffeners is desirable because their presence increases the likelihood that local buckling of the beam top flange would occur outside the haunch region, not next to the column face (i.e., location of groove weld).

The beam web together with a pair of transverse stiffeners should also be checked in accordance with Chapter K of the AISC's Load and Resistance Factor Design (LRFD) Specification (Load 1993) for local flange bending, local web yielding, and web crippling to ensure that the strength is sufficient to resist a concentrated force of βV_{pd} .

Continuity Plates

Whenever possible, it is desirable to add a pair of continuity plates at the beam top flange level to reduce the stress concentration in the groove weld. A pair of continuity plates should be added at the location where the haunch flange intersects the column. The continuity plates, designed for a concentrated force of $\beta V_{pd}/\tan \theta$, should satisfy the requirements in Chapter K of the LRFD Specification (Load 1993).

SUMMARY OF WELDED HAUNCH DESIGN PROCEDURE

The step-by-step design procedure for a welded haunch connection is summarized as follows (a design example is presented in Appendix I):

- Step 1: Select a preliminary haunch geometry using (22) and (23).
- Step 2: Compute the beam design plastic moment (24) and beam shear (26).
- Step 3: Check for strong column-weak beam condition (27).
- Step 4: Compute the required β_{\min} value (17) to limit the top flange groove weld stress to an allowable value ($0.8 F_{EXX}$).
- Step 5: Select a haunch section such that the haunch flange satisfies (18) for strength and (19) for compactness. The haunch web needs to satisfy (21) for strength and (20) for compactness.
- Step 6: Use (8) to compute the actual β value and check whether the haunch flange has a sufficient stiffness to develop the required β in (17). Increase the haunch flange area or modify the haunch geometry if β is less than β_{\min} . The designer may consider reducing the haunch flange area if β is significantly larger than β_{\min} .
- Step 7: Use (29) to check the shear capacity of the existing beam web connection.
- Step 8: Design the continuity plates and the beam web stiffeners based on the actual β value.

CONCLUSIONS

The main conclusions can be summarized as follows:

1. Based on the satisfactory full-scale cyclic testing results of two-sided pre-Northridge steel moment connections that were rehabilitated with welded haunch beneath the beams, it was found in this NIST/AISC research program that this scheme is a feasible solution for seismic rehabilitation. When the composite slab was present, haunch connections were able to deliver a plastic rotation on the order of 0.03 rad with no fracture at the existing beam flange welded joints.
2. The presence of a welded haunch dramatically changes the beam shear force transfer mechanism. Conventional beam theory cannot provide a reliable prediction of stress distributions in the haunch connection. Both theoretical studies and experimental results have shown that the majority of the beam shear is transferred to the column through the haunch flange rather than through either the beam web bolted connection or the beam flange groove welds. This strut action alters the moment distribution of the beam in the haunch region.
3. Providing sufficient axial stiffness and strength to the haunch flange, the force demand in the existing bottom flange groove weld is significantly reduced, and the force demand in the existing top flange groove weld can be reduced to a reasonable level. The haunch web has a minor effect on the flexural stress distribution in the beam. But it is needed to stabilize the haunch flange.
4. A simplified model that considers both force interaction and deformation compatibility between the beam and the haunch was developed. The predicted beam flexural stress distribution near the column face correlated well with the finite-element analysis results. The model could also be used to explain the "reverse" beam shear phenomenon that was observed in testing. Based on the simplified model, a step-by-step design procedure is proposed. The design procedure is also applicable to new design.

APPENDIX I. DESIGN EXAMPLE

Description of Existing Frame

- Building constructed in early 1980's.
- Frame Centerline Dimensions:
Story Height: $H_c = 3,657.6$ mm (12 ft)
Beam: W36×150, A36 steel
Bay Width: $L = 9,144$ mm (30 ft)
Column: W14×426, A572 Grade 50 steel
- Pre-Northridge Moment Connection Details: (1) Welded flange-bolted web moment connection; (2) beam flange groove welds: E70T-4 flux-cored arc welding with steel backing and weld tab left in place; (3) beam web connection: nine 25 mm (1 in.) diameter A325 high strength bolts, $16 \times 127 \times 699$ mm ($5/8 \times 5 \times 27$ 1/2 in.) shear plate connected to the column with 8 mm (5/16 in.) fillet welds, no supplemental web welds between the shear plate and the beam web; (4) no continuity plates; and (5) no doubler plates.

Member Section Properties

- W36×150 Beam: $d = 910.6$ mm (35.85 in.); $b_{hf} = 304.1$ mm (11.975 in.); $t_{bf} = 23.9$ mm (0.94 in.); $t_{bw} = 15.9$ mm (0.625 in.); $A_b = 28,516.0$ mm² (44.2 in.²); $I_x = 3,762,732,087$ mm⁴ (9,040 in.⁴); and $Z_{bx} = 9,520,884.2$ mm³ (581 in.³)

- W14×426 Column: $d_c = 474$ mm (18.67 in.); $t_{cw} = 47.6$ mm (1.875 in.); $t_{cf} = 83.9$ mm (3.305 in.); $b_{cf} = 424.1$ mm (16.695 in.); and $Z_{cx} = 14,240,358.6$ mm³ (869 in.³)

Connection Modification Design

Consider a uniformly distributed gravity load [$w_g = 8.76$ kN/m (6 kip/ft)] for the beam. Assume a column axial stress f_a of 68.9 MPa (10 ksi).

Step 1: Select preliminary haunch dimensions as follows:

$$A = (0.5 \text{ to } 0.6)d_b \quad \text{Choose } a = 457.2 \text{ mm (18 in.)}$$

$$\theta = 30^\circ \pm 5^\circ \quad \text{Choose } \theta = 31^\circ$$

$$b = a \tan \theta = 274.3 \text{ mm (10.8 in.)}$$

Step 2: Determine beam probable plastic moment M_{pd} and beam shear V_{pd}

$$F_{ye} = 1.3F_y = 1.3(248) = 322.6 \text{ MPa (46.8 ksi)}$$

$$M_{pd} = \alpha Z_{bx} F_{ye} = 1.1 \times 9,520,884.2 \times 322.6$$

$$= 3,378,581 \text{ kN-mm (29,910 kip-in.)}$$

$$L' = 9,144 - 224.0 - 2 \times 457.2 = 8,005.6 \text{ mm (305.3 in.)}$$

$$V_{pd} = \frac{2M_{pd}}{L'} + \frac{w_g L'}{2} = 905.2 \text{ kN (203.5 kips)}$$

Step 3: Check for strong column-weak beam condition

$$\sum M_c = [2M_{pd} + V_{pd}(L - L')] \left(\frac{H_c - d_p}{H_c} \right)$$

$$= 5,419,176 \text{ kN-mm (47,966 kip-in.)}$$

$$\frac{\sum Z_c(F_{yc} - f_a)}{\sum M_c} = 1.45 > 1.0 \quad \text{OK}$$

Step 4: Determine β_{min} . Use (17) to compute the required β , where $F_w = 0.8F_{EXX} = 386.1$ MPa (56 ksi)

$$\beta_{min} = \frac{(M_{pd} + V_{pd}a)/S_x - F_w}{\frac{V_{pd}a}{S_x} + \frac{V_{pd}}{I_b \tan \theta} \left(\frac{d^2}{4} - \frac{I_b}{A_b} \right)} = 0.91$$

Step 5: Size haunch flange. Use (18) to size haunch flange for strength

$$A_{hf} \geq \frac{P_{hf}}{\phi F_y} = \frac{\beta V_{pd}}{\phi F_y \sin \theta} = 5,154.8 \text{ mm}^2 (7.99 \text{ in.}^2)$$

Select W18×86 (A572 Grade 50 steel), which provides a haunch flange area of 5,509.7 mm² (8.54 in.²) [$=b_{hf} \times t_{hf} = 281.7 \times 19.6$ mm (11.09×0.77 in.)]. Check (19) for the compact section requirement

$$\frac{b_{hf}}{2t_{hf}} = \frac{281.7}{2(19.6)} = 7.2 \leq \frac{137}{\sqrt{F_y}} = 7.38 \quad \text{OK}$$

Step 6: Verify the β value for stiffness requirement. Use (8) to compute the actual β value for the haunch flange stiffness requirement

$$\beta = \frac{b}{a} \left(\frac{3L'd + 3ad + 3bL' + 4ab}{3d^2 + 6bd + 4b^2 + \frac{12I_b}{A_b} + \frac{12I_b}{A_{hf} \cos^3 \theta}} \right) = 0.93 > \beta_{min} \quad \text{OK}$$

The haunch, thus sized, would ensure that the tensile stress in the top flange groove weld is limited to the allowable stress $F_w = 386.1$ MPa (56 ksi). The tensile stress in the top flange groove weld can be computed from (9)

$$f_{wr} = \frac{M_{pd} + V_{pd}(1 - \beta)a}{I_b} \left(\frac{d}{2} \right) - \frac{\beta V_{pd} \tan \theta}{I_b} \left(\frac{d^2}{4} - \frac{I_b}{A_b} \right)$$

$$= 384.0 \text{ MPa (55.7 ksi)} < 386.1 \text{ MPa (56 ksi)} \quad \text{OK}$$

The haunch flange axial stress is

$$\frac{\beta V_{pd}}{A_{hf} \sin \theta} = \frac{0.93 \times 905.2}{5,509.7 \times 0.515} = 296.4 \text{ MPa (43 ksi)} < \phi F_y$$

$$= 310.2 \text{ MPa (45 ksi)} \quad \text{OK}$$

where $\phi = 0.9$. Therefore, the selected haunch flange has adequate stiffness and strength.

The maximum tensile stress in the groove weld of the beam bottom flange can be computed from (11)

$$f_{wb} = \frac{V_{pd}L'/2 + V_{pd}(1 - \beta)a}{I_b} \left(\frac{d}{2} \right) - \frac{(\beta V_{pd} \tan \theta)}{I_b} \left(\frac{d^2}{4} + \frac{I_b}{A_b} \right)$$

$$= 286.1 \text{ MPa (41.5 ksi)} < 386.1 \text{ MPa (56 ksi)} \quad \text{OK}$$

Step 7: Check haunch web and beam web shear capacities. Use (20) to check the haunch web width-thickness ratio

$$\frac{a \sin \theta}{t_{hw}} = \frac{457.2 \sin 31^\circ}{12.2} = 19.3 \leq \frac{683}{\sqrt{F_y}} = 36.8 \quad \text{OK}$$

The average shear stress in the haunch web can be computed using (20)

$$\tau_{hw} = \frac{aV_{pd}}{2(1 + \nu)I_b} \left(\frac{L'}{2} - \frac{\beta}{\tan \theta} \left(\frac{d}{2} \right) + \frac{(1 - \beta)a}{3} \right)$$

$$= 134.5 \text{ MPa (19.5 ksi)} < \phi(0.6F_y) = 186.2 \text{ MPa (27 ksi)} \quad \text{OK}$$

Use (29) to compute the shear in the beam web

$$V_{bw} = (1 - \beta)V_{pd} = (1 - 0.93) \times 905.2 = 63.2 \text{ kN (14.2 kips)}$$

The above computation indicates that the welded haunch is very effective in reducing the beam shear at the column face. Nine existing high strength bolts [25.4 mm (1 in.) diameter A325 bolts] can provide a shear strength of 536.4 kN (120.6 kips).

Step 8: Design welds and stiffeners. Complete penetration groove weld [E71T-8 electrode with a specified CVN value of 27.1 J (20 ft-lb) at -28.8°C (-20°F)] at both ends of the haunch flange are specified to transmit the haunch flange force.

Design the haunch web fillet weld (30)

$$V_{hw} = \tau_{hw}t_{hw} = 134.5 \times 12.2 = 1.64 \text{ kN/mm (9.4 kips/in.)}$$

The required fillet weld size is

$$a_w \geq \frac{V_{hw}}{\phi(0.707)(0.60F_{yw})2} = 5.3 \text{ mm (0.21 in.)}$$

An 8 mm (5/16 in.) fillet weld size on both sides of the haunch web is sufficient.

Without beam web vertical stiffeners, the maximum concentrated compressive strength is governed by local web yielding (Load 1993)

$$\phi R_n = 1.0(2.5k + N)F_{yw}t_w = 758.4 \text{ kN (170.5 kips)} < \beta V_{pd}$$

$$= 842.0 \text{ kN (189.3 kips)} \quad \text{NG}$$

Try a pair of $12.7 \times 133.4 \text{ mm}$ ($1/2 \times 5 \text{ 1/4 in.}$) plates (A572 Grade 50 steel) for the stiffeners. Check the width-thickness ratio

$$\frac{b}{t} = \frac{133.4}{12.7} = 10.5 \leq \frac{250}{\sqrt{F_y}} = 13.4 \quad \text{OK}$$

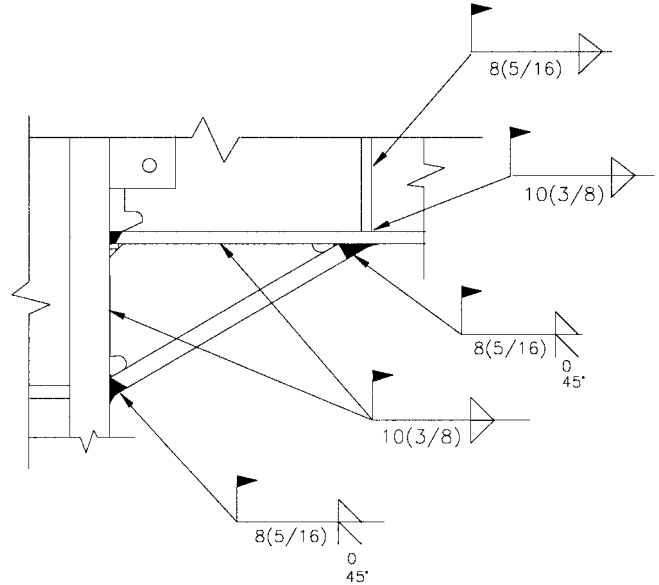


FIG. 13. Typical Haunch Welding Details

Treat the stiffened web as an axially compressed member with an effective length of $0.75h$ [$h = 825.5 \text{ mm}$ (32.5 in.)], a cross section composed of two stiffeners and a strip of the beam web having a width of $12t_w$ (Load 1993)

$$A_{eff} = 2(133.4)(12.7) + 12(15.9)(15.9) = 645.2 \text{ mm}^2 (9.94 \text{ in.}^2)$$

$$I_{eff} = 12.7(133.4 \times 2 + 15.9)^2/12 = 23,891,683.8 \text{ mm}^4 (57.4 \text{ in.}^4)$$

$$r = \sqrt{\frac{I_{eff}}{A_{eff}}} = \sqrt{\frac{23,891,683.8}{645.2}} = 61 \text{ mm (2.4 in.)}$$

$$\frac{KL}{r} = \frac{0.75h}{r} = \frac{0.75(825.5)}{61} = 10.2$$

$$\phi_c F_{cr} = 291 \text{ MPa (42.2 ksi)}$$

$$\phi_c P_n = \phi_c F_{cr}(A_{eff}) = 291 (645.2) = 1,863.7 \text{ kN (419 kips)} > \beta V_{pd}$$

$$= 842 \text{ kN (189.3 kips)} \quad \text{OK}$$

Use complete joint penetration groove weld to connect each stiffener to the beam flange. Use two-sided 8 mm (5/16 in.) fillet welds to connect the stiffeners to the beam web. Fig. 13 shows the welding details.

ACKNOWLEDGMENTS

This paper presents part of a research project funded by NIST, Gaithersburg, Md., under Grant No. 70NANB5H0126. Additional financial support was provided through AISC, Chicago, by the Northridge Steel Industry Fund. The writers would like to thank the AISC reviewers and Roy Becker for their comments on the design procedure.

APPENDIX II. REFERENCES

- ABAQUS user's manual, vols. I and II. (1995). Version 5.6, Hibbit, Karlsson & Sorenson, Inc., Providence, R.I.
- Civjan, S. A., and Engelhardt, M. D. (1998). "Experimental investigation of methods to retrofit connections in existing seismic-resistant steel moment frames." *Summary Final Rep. to the National Institute of Standards and Technology*, Phil M. Ferguson Struct. Engrg. Lab., University of Texas at Austin, Austin, Tex.
- El-Tawil, S., Mikesell, T., Vidarsson, E., and Kunnath, S. K. (1998). "Strength and ductility of FR welded-bolted connections." *Rep. No. SAC/BD-98/01*, SAC Joint Venture, Sacramento, Calif.
- Galambos, T. V., and Ravindra, M. K. (1978). "Properties of steel for use in LRFD." *J. Struct. Div.*, ASCE, 104(9), 1459-1468.
- Goel, S. C., Stojadinovic, B., and Lee, K.-H. (1997). "Truss analogy for steel moment connections." *Engrg. J.*, 34(2), 43-53.

Gross, J. L., Engelhardt, M. D., Uang, C.-M., Kasai, K., and Iwankiw, N. (1999). "Modification of existing welded moment frame connections for seismic resistance." *Steel Design Guide Series 12*, AISC, Chicago.

"Interim guidelines: Evaluation, repair, modification and design of welded steel moment frame structures." (1995). *FEMA267*, SAC Joint Venture, Sacramento, Calif.

Lee, C. H., and Uang, C.-M. (1997). "Analytical modeling of dual panel zone in haunch repaired steel MRFs." *J. Struct. Engrg.* ASCE, 123(1), 20–29.

Load and Resistance Factor Design (LRFD) Specification. (1993). 2nd Ed., AISC, Chicago.

Popov, E. P., and Stephen, R. M. (1972). "Cyclic loading of full-size steel connections." *Bull. No. 21*, American Iron and Steel Institute, Washington, D.C.

Ramm, E. (1981). "Strategies for tracing the nonlinear response near limit points." *Nonlinear finite element analysis in structural mechanics*, E. Wunderlich, E. Stein, and K. J. Bathe, eds., Springer, Berlin.

SAC. (1996). "Technical report: Experimental investigations of beam-column subassemblies." *Rep. No. SAC-96-01*, SAC Joint Venture, Sacramento, Calif.

Seismic provisions for structural steel buildings. (1997). 2nd Ed., AISC, Chicago.

Uang, C.-M., Yu, Q.-S., Noel, S., and Gross, J. (2000). "Cyclic testing of steel moment connections rehabilitated with RBS or welded haunch." *J. Struct. Engrg.*, ASCE, 126(1), 57–68.

Uniform building code. (1985). International Conference of Building Officials, Whittier, Calif.

Youssef, N., Bonowitz, D., and Gross, J. (1995). "A survey of steel moment-resisting frame buildings affected by the 1994 Northridge earthquake." *Rep. No. NISTIR 5625*, NIST, Gaithersburg, Md.

Yu, Q.-S., Noel, S., and Uang, C.-M. (1997). "Experimental and analytical studies on seismic rehabilitation of pre-Northridge steel moment connections: RBS and haunch approaches." *Rep. No. SSRP-97/08*, Div. of Struct. Engrg., University of California at San Diego, La Jolla, Calif.

APPENDIX III. NOTATION

The following symbols are used in this paper:

A_b = area of beam section;
 A_{hf} = haunch flange area;
 a = length of welded haunch;
 a_w = fillet weld size;
 b = depth of welded haunch;
 b_{hf} = haunch flange width;
 d = beam depth;
 d_c = column depth;
 d_p = depth of modified beam (i.e., includes haunch);
 E = Young's modulus [199,955 MPa (29,000 ksi)];
 F_{EXX} = strength of weld metal [MPa (ksi)];
 F_u = specified minimum tensile strength of steel [MPa (ksi)];
 F_w = allowable tensile stress of groove weld ($0.8F_{EXX}$)
 F_y = specified minimum yield strength of steel [MPa (ksi)];

F_{yc} = minimum specified yield of column;
 F_{ye} = expected yield strength of steel [MPa (ksi)];
 f_a = axial stress in column above and below;
 f_{wb} = tensile stress at beam bottom flange groove weld;
 f_{wt} = tensile stress at beam top flange groove weld;
 H_c = story height;
 I_b = moment of inertia of beam section;
 I_{hb} = moment of inertia of beam section including haunch;
 k = haunch flange axial stiffness;
 L = center-to-center spacing of columns;
 L' = beam span between plastic hinges;
 l_{hf} = haunch flange length;
 M_{pd} = design plastic moment of beam at haunch tip;
 P_{bf} = beam bottom flange force;
 P_{hf} = haunch flange force;
 R_y = ratio of expected yield strength F_{ye} to specified minimum yield strength F_y ;
 t_{bf} = beam flange thickness;
 t_{bw} = beam web thickness;
 t_{cf} = column flange thickness;
 t_{cw} = column web thickness;
 t_{hf} = haunch flange thickness;
 t_{hw} = haunch web thickness;
 u_B = horizontal displacement of beam bottom flange at haunch tip;
 $u(x)$ = horizontal displacement field of haunch web;
 V_{bw} = shear force in beam web;
 V_c = shear force in column above and below connection;
 V_G = beam shear force due to gravity loads;
 V_{pd} = design beam shear force;
 v_B = vertical displacement of beam bottom flange at haunch tip;
 $v(x)$ = vertical displacement field of haunch web;
 w_g = uniform beam load;
 Z_b = plastic section modulus of beam section;
 Z_c = plastic section modulus of column section;
 α = strain hardening factor of steel;
 β = ratio of vertical component of haunch flange force to design shear force V_{pd} ;
 β_{min} = minimum β value to limit beam top flange groove weld stress to F_w ;
 γ_{hw} = shear strain of haunch web;
 δ_h = axial shortening of haunch flange;
 θ = acute angle between haunch flange and beam flange;
 θ_p = plastic hinge rotation;
 ν = Poisson's ratio of steel (0.3);
 $\sigma(x)$ = compressive stress in beam bottom flange;
 τ_{hw} = haunch web shear stress;
 ϕ, ϕ_v = resistance factor; and
 ΣM_c = sum of column moment at top and bottom of enlarged panel zone.